Altered properties of quantal neurotransmitter release at endplates of mice lacking P/Q-type Ca^{2+} channels

Francisco J. Urbano*†, Erika S. Piedras-Rentería‡§, Kisun Jun¶, Hee-Sup Shin‖, Osvaldo D. Uchitel*, and Richard W. Tsien‡

‡Department of Molecular and Cellular Physiology, Stanford University School of Medicine, Stanford, CA 94305; *Laboratorio de Fisiología y Biología Molecular y Celular, Facultad de Ciencias Exactas y Naturales, Universidad de Buenos Aires, Ciudad Universitaria, Pabellón II-2do piso, (C1428EHA)-Buenos Aires, Argentina; ¶Cell and Gene Therapy Research Institute, College of Medicine, Pochon CHA University, Seoul 198-1, Korea; and ‖National CRI Center for Calcium and Learning, Korea Institute of Science and Technology, Seoul 130-650, Korea

Contributed by Richard W. Tsien, December 30, 2002

Transmission at the mouse neuromuscular junction normally relies on P/Q-type channels, but became jointly dependent on both N- and R-type Ca^{2+} channels when the P/Q-type channel α_{1A} subunit was deleted. R-type channels lay close to Ca^{2+} sensors for exocytosis and $I_{K(Ca)}$ channel activation, like the P/Q-type channels they replaced. In contrast, N-type channels were less well localized, but abundant enough to influence secretion strongly, particularly when action potentials were prolonged. Our data suggested that active zone structures may select among multiple Ca^{2+} channels in the hierarchy P/Q>R>N. The $\alpha_{1A}-/-$ neuromuscular junction displayed several other differences from wild-type: lowered quantal content but greater ability to withstand reductions in the Ca^{2+}/Mg^{2+} ratio, and little or no paired-pulse facilitation, the latter findings possibly reflecting compensatory mechanisms at individual release sites. Changes in presynaptic function were also associated with a significant reduction in the size of postsynaptic acetylcholine receptor clusters.

neuromuscular junction | α_{1A} knockout | paired-pulse facilitation | SNX-482 | Ca^{2+}-activated potassium channel

The relationship between voltage-gated calcium channels and Ca^{2+} sensors for exocytosis lies at the heart of excitation–secretion coupling yet is incompletely understood. New molecular approaches can now be applied using mice that lack key protein components responsible for synaptic transmission (1–5). What would happen to neurotransmission if the Ca^{2+} channels that normally trigger vesicular fusion were removed? The dominant Ca^{2+} entry mechanism for synaptic communication at most synapses is the Ca^{2+} channel known as P/Q-type (6–9). These channels are generated by the pore-forming α_{1A} subunit (10) ($Ca_V2.1$) (11) with support from ancillary subunits ($\alpha_2\delta$ and β) and engage in close interactions with molecular components of the exocytotic machinery. The generation of α_{1A}-null mutant mice allows a critical examination of what features of neurotransmission depend on P/Q-type channels (12, 13). Elimination of P/Q calcium channels induces a rapidly progressive neurological syndrome $\approx$10 days after birth, characterized by loss of balance and twisting movements of limbs, including extensor spasms of the hind legs consistent with dystonia. The falling episodes and ataxia increase with age until the mice are unable to walk and die [approximately postnatal day (P) 20]. The display of ataxia and dystonia by the $\alpha_{1A}-/-$ mice underscores the importance of α_{1A} for normal function of the central nervous system, relevant to human diseases arising from defects in this subunit, including certain forms of migraine, epilepsy and ataxia (14, 15).

The neuromuscular junction (NMJ) is an interesting system for examining the impact of removing α_{1A}, having been the focus of pioneering work on the quantal nature of transmission (16), the steep dependence of transmitter release on Ca^{2+} entry (17), the fine structure of the presynaptic terminal (18–20), and many other features of synapses (21, 22). At mature mammalian endplates, P/Q-type Ca^{2+} channels are wholly responsible for the control of acetylcholine release (23–27). What happens to synaptic transmission at the NMJ if P/Q-type channels are deleted? Various outcomes are possible: (*i*) Neurotransmission might be greatly deranged because specific Ca^{2+} channels play a critical structural role in organizing the presynaptic release machinery (20, 28), or in correctly aligning presynaptic release sites and postsynaptic receptors (29, 30). (*ii*) Neurotransmission might not change at all if other Ca^{2+} channel types substituted perfectly for P/Q-type channels, a plausible outcome given the highly homologous structure of multiple Ca^{2+} channel types (31), which jointly support transmitter release at many CNS synapses (32–35). (*iii*) In an intermediate outcome, basic features of neuromuscular transmission might be retained, but with significant changes in the relationship between Ca^{2+} entry and downstream responses such as transmission or short-term plasticity.

To test these ideas, we carried out an extensive comparison of the properties of neuromuscular transmission at endplates of wild-type (WT) and $\alpha_{1A}-/-$ mice. Although the α_{1A}-deficient NMJ were morphologically intact at the light microscopic level, and displayed miniature endplate potentials (MEPPs) with amplitudes indistinguishable from WT junctions, several aspects of synaptic transmission were significantly altered. Quantal transmitter release became jointly dependent on N-type and R-type channels in the $\alpha_{1A}-/-$, with different susceptibility to internal Ca^{2+} buffering and relationship to Ca^{2+}-activated potassium channels when these channel types acted individually. These results suggested that Ca^{2+} channels differ markedly in their ability to interact with the exocytotic release machinery. Strikingly, paired-pulse facilitation was almost completely abolished.

Materials and Methods

Reagents were purchased from Sigma (analytical grade), except when noted. SNX 482 was a kind gift from Elan Pharmaceuticals.

Muscle Dissection. All animal handling was in accord with guidelines of the Animal Care and Use Committee. Mice were anesthetized with isoflurane (AErrane, Baxter Health Care, Mundelein, IL) and immediately exsanguinated. The phrenic

Abbreviations: NMJ, neuromuscular junction; MEPP, miniature endplate potential; EPP, evoked endplate potential.

†Present address: Department of Physiology and Neuroscience, New York University School of Medicine, 550 First Avenue, New York, NY 10016.

§Present address: Department of Cellular and Molecular Physiology, Loyola University Chicago, Maywood, IL 60153.

**To whom correspondence should be addressed. E-mail: rwtsien@stanford.edu.

nerve-diaphragm or the levator auris longus muscle were excised and dissected in physiological saline solution containing 150 mM NaCl, 5 mM KCl, 2 mM $CaCl_2$, 1 mM $MgCl_2$, 10 mM Hepes, 11 mM glucose (pH 7.4), and continuously bubbled with O_2. All experiments were performed at room temperature.

Electrophysiology. Evoked endplate potentials (EPPs) and spontaneous MEPPs were recorded with conventional intracellular microelectrodes filled with 3 M KCl (20–30 MΩ). After muscle impalement, the phrenic nerve was stimulated with two platinum electrodes coupled to a stimulus isolation unit (Isolator-11, Axon Instruments). If necessary, μ-conotoxin GIIIB (1 μM, Alomone, Jerusalem) was used to prevent muscle contraction. Neurotransmitter release was evaluated at high and low $[Ca^{2+}]/[Mg^{2+}]$ ratios, where the mean quantal content (m) was obtained, respectively, by the coefficient of variation and failure methods (36).

MEPPs were recorded in physiological saline solution for periods of 1–2 min. EPPs and MEPPs amplitudes were obtained from cells with stable resting potentials and corrected to a resting potential of −75 mV (37).

Facilitation of Transmitter Release. Paired responses were elicited by supramaximal twin-pulse nerve stimuli. Facilitation index (V_2/V_1) was obtained by comparing second and first EPPs averaged over 16 trials. When trains of 10 stimuli (100 Hz) were applied, the train index was defined as $[(V_9+V_{10})/2]/V_1$, where V_n was the nth EPP of the train, averaged over 16 trials.

Cell-Permeant Buffer Loading. Muscles were incubated in a Ca^{2+}-free saline solution in the presence of EGTA-AM or DM-BAPTA-AM (Molecular Probes) or dimethyl sulfoxide, as described (38).

Pre- and Postsynaptic Staining. Presynaptic labeling was obtained by incubation with 8 μM FM1–43 for 15 min in a modified physiological solution containing 45 mM KCl, followed by three washes (10 min each) in physiological saline. Postsynaptic acetylcholine receptors were stained for 30 min in saline solution supplemented with 0.1 nM Texas red-conjugated α-bungarotoxin (Molecular Probes). Three-dimensional NMJ reconstructions from 20 sections (1 μm each) along the Z axis were obtained with an MDI 2010 confocal microscope (Molecular Dynamics). Postsynaptic areas were quantified by using NIH IMAGE.

Presynaptic Perineurial Recordings. Perineurial currents are proportional to the conductance changes at synaptic terminals and were monitored as voltage drops across the perineurial resistance (39, 40). Presynaptic perineurial calcium-activated potassium currents $I_{K(Ca)}$ were recorded in Levator auris muscles in the presence of 30 μM d-tubocurarine and 2 mM 3,4-diaminopyridine to block postsynaptic acetylcholine receptor and voltage-activated K^+ channels (39, 40).

Statistics. Data are expressed as the mean ± SEM. Statistical significance was evaluated by using two-tailed Student's t test. When appropriate, nonparametric Kolmogorov–Smirnov and median tests for unmatched pairs were used.

Results

Morphology. To determine whether the absence of P/Q-type channels affects overall synaptic morphology, we examined pre- and postsynaptic markers at NMJs of the levator auris longus and diaphragm muscles. NMJs of WT and knockout mice were able to take up the styryl dye FM1–43 (41) in an activity-dependent manner, indicating that exo/endocytotic cycling of presynaptic vesicles was functional (data not shown). Although smaller in size, there was no obvious difference in the overall morphology of the $\alpha_{1A}-/-$ nerve terminal. Postsynaptic clusters of acetylcholine receptors were identified by staining with α-bungarotoxin conjugated with Texas red (Fig. 1*A*). Acetylcholine receptor-labeled clusters in diaphragms of $\alpha_{1A}-/-$ mice showed a significant reduction in size, from 189 ± 15 μm^2 in WT (n = 52, 3 mice) to 112 ± 14 μm^2 (n = 22, 4 mice) (Fig. 1*B*, $P < 0.001$).

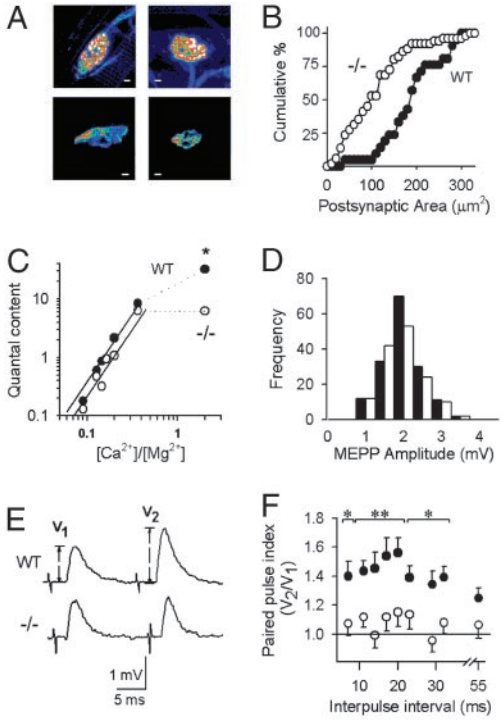

Fig. 1. Morphology and neurotransmission at WT and $\alpha_{1A}-/-$ NMJs. Filled symbols, WT; open symbols, $-/-$. (*A*) NMJs from WT (*Left*) and $\alpha_{1A}-/-$ (*Right*) mice stained with FM1–43 (*Upper*) and α-bungarotoxin (*Lower*) as pre- and postsynaptic markers. [Scale bars: 10 μm (*Upper Left*) and 5 μm (all others).] (*B*) Cumulative distributions of postsynaptic site areas are smaller in the $-/-$ ($P < 0.001$). (*C*) Double-logarithmic plot of quantal content vs. $[Ca^{2+}]_o/[Mg^{2+}]_o$. At low $[Ca^{2+}]/[Mg^{2+}]$ ratios, data were fitted with a linear equation where the slope of the plot was 2.7 for both WT and $-/-$ NMJs (continuous lines) ($r^2 > 0.9$). Quantal content values at high $[Ca^{2+}]/[Mg^{2+}]$ were significantly different (**, $P < 0.001$). (*D*) MEPP amplitude distribution histograms. (*E*) Averaged traces of EPPs evoked by a 17-ms paired pulse stimulation (*Upper*, WT; *Lower*, $-/-$). (*F*) Paired pulse index (*, $P < 0.05$; **, $P < 0.001$).

Evoked and Spontaneous Neurotransmitter Release. Spontaneous MEPP amplitudes averaged 1.8 ± 0.1 mV for WT and 1.7 ± 0.2 mV for $-/-$ in normal saline solution (n = 158 and 143, $P > 0.3$) (Fig. 1*C*), indicating that quantal size was not affected by the absence of P/Q-type channels. In contrast, MEPP frequency was significantly different, 25 ± 3 min^{-1} for WT (n = 35) and 11 ± 2 min^{-1} for $\alpha_{1A}-/-$ NMJs (n = 48) ($P < 0.001$). Exposure to depolarizing solution (15 mM K^+) led to an increase in MEPP frequencies, to 320 ± 45 min^{-1} in WT (n = 35) and 136 ± 10 min^{-1} in $\alpha_{1A}-/-$ (n = 51) ($P < 0.001$). The lower frequency of minis observed in the $\alpha_{1A}-/-$ may be in line with the reduced size of their NMJ.

Clear differences between $-/-$ and WT NMJ were observed in nerve-evoked EPPs recorded with external solution containing 2 mM $[Ca^{2+}]_o$ and 1 mM $[Mg^{2+}]_o$ (Fig. 1*D*). Here quantal content was 32 ± 3 at WT NMJ (n = 25), but only 6.2 ± 0.5 at $-/-$ endplates (n = 20) ($P < 0.001$). Further recordings were carried out with $[Ca^{2+}]_o$ varied between 0.5–2 mM and $[Mg^{2+}]_o$ held fixed at 5.5 mM (Fig. 1*D*). Over this range of low $[Ca^{2+}]/$

$[Mg^{2+}]$ ratios, m increased steeply with elevations in that ratio, with a slope of 2.7 in both WT and $-/-$ ($r^2 > 0.9$). No significant differences were observed in the vertical intercepts in a log–log plot ($P > 0.5$), in clear contrast to the 5-fold vertical displacement with $[Ca^{2+}]/[Mg^{2+}] = 2$.

Our analysis of endplate morphology and electrophysiology suggest that (*i*) P/Q-type channels were not essential for the establishment of functional pre- and postsynaptic elements of the NMJ, but their deletion caused a decrease in postsynaptic areas and a sharp drop of quantal content and mini frequency in physiological saline (high $[Ca^{2+}]/[Mg^{2+}]$ ratio), consistent with fewer release sites. (*ii*) The steep dependence of transmission on $[Ca^{2+}]_o$ was maintained, excluding the notion that α_{1A} might be directly and uniquely involved in Ca^{2+} sensing. (*iii*) Under conditions of low $[Ca^{2+}]/[Mg^{2+}]$ and meager release probability, the quantal content was remarkably preserved despite the absence of α_{1A}. If the sharp decrease of quantal content in normal saline reflected a loss of working release sites, there may have been a compensatory increase in release probability at individual sites to maintain overall quantal content in low $[Ca^{2+}]/[Mg^{2+}]$.

Short-Term Plasticity. At the WT NMJ, paired stimulation in low $[Ca^{2+}]/[Mg^{2+}]$ solutions consistently produced paired-pulse facilitation (PPF) (42, 43). The amplitude of the second EPP was typically 40% greater than that of the first response after a rest period (Fig. 1*E*). In striking contrast, little or no PPF was observed in $-/-$ NMJs, averaging only ≈10%. Pooled data for the PPF index (Fig. 1*F*) showed a significant difference between WT and $-/-$ NMJ at all inter-pulse intervals between 7 to 55 ms except the longest one. To test whether a Ca^{2+} sensor for short-term facilitation might specifically require the presence of α_{1A}, we examined potentiation on application of a high-frequency train to greatly raise intracellular Ca^{2+} (data not shown). With this form of stimulation, the cumulative facilitation in the $-/-$NMJ recordings (see *Materials and Methods*) was substantial, averaging 75 ± 26% above control, although significantly less than the average train index for WT NMJ, 165 ± 13% ($P < 0.001$).

Identification of Ca^{2+} Channels Supporting Transmission at $\alpha_{1A}-/-$ Synapses. The virtual absence of PPF at synapses lacking α_{1A} raised interesting questions about the Ca^{2+} channels that support neurotransmission in the absence of P/Q-type. We performed a pharmacological analysis of the Ca^{2+} channel types that support transmitter release at WT and $-/-$ NMJs (Fig. 2*A*). We used a conventional panel of type-specific blockers to block P/Q-, N-, R-, and L-type channels, respectively, ω-agatoxin-IVA (Aga IVA, 100 nM), ω-conotoxin GVIA (GVIA, 3 μM), SNX-482 (1 μM) and nimodipine (nimo, 10 μM). The average reduction of quantal content by the inhibitors was expressed as a percentage of control. At the WT NMJ (Fig. 2*A*, filled bars), block by Aga IVA was virtually complete (98 ± 1%) and also irreversible; blockers of other channels showed little or no effect. On the contrary, at the NMJ of $-/-$ mice (open bars), Aga IVA had no significant effect (6 ± 6%), whereas quantal content was significantly reduced by GVIA (82 ± 3%), by SNX-482 (72 ± 6%), and by both blockers applied together (95 ± 1%). Nimodipine did not significantly affect quantal content at either WT NMJ (6.6 ± 3.1%) or $-/-$ NMJ (−6.4 ± 9.4%).

Block by SNX-482 was readily reversible at all levels tested. The inhibition was steeply dependent on SNX-482 concentration, with no significant block at 0.3 μM, >50% block at 0.42 μM, and essentially complete block at 0.5 μM (Fig. 2 *B* and *C*). The midpoint concentration was 10-fold higher than for SNX-482 block of cloned α_{1E} channels (44), possibly reflecting differences in α_{1E} splice variants (44–46). The extreme steepness of the dose–response curve for neurotransmission differs from the conventional 1:1 curve found for block of Ca^{2+} channels (44). The simplest interpretation is that under the conditions used for quantal analysis, synaptic transmission at $-/-$ NMJ depended on the opening of two or more SNX-482-sensitive Ca^{2+} channels. This fits nicely with inferences based on the nonadditive actions of maximally effective concentrations of SNX-482 and GVIA. Both lines of evidence supported the idea that vesicular fusion is triggered by the concerted action of multiple Ca^{2+} channels, whether they are of the same type or different types.

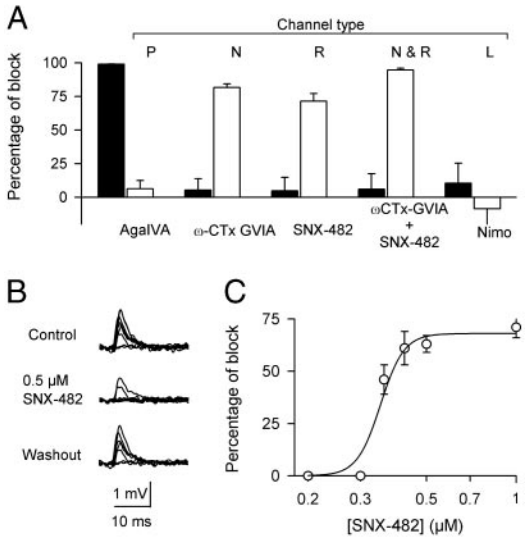

Fig. 2. Pharmacological dissection of calcium channels supporting neurotransmitter release in the α_{1A} $-/-$ NMJ. (*A*) Quantal content in the presence of blockers for the P/Q-(200 nM AgaIVA), N- (GVIA, 3 μM), R- (1 μM SNX 482), and L-type calcium channel (10 μM Nimo) for WT (filled bars) and $-/-$ NMJ (open bars) (n = 16–33). (*B*) Reversibility of SNX-482 block. Representative EPPs recorded in $-/-$ during nerve stimulation (control), + 0.5 μM SNX 482, and after 45-min washout. Stimulation artifacts were reduced for clarity. (*C*) Dose–response curve for SNX 482 in the mutant NMJ (IC_{50} = 347 ± 12 nM).

N-Type Ca^{2+} Channels Are More Distant from Ca^{2+} Sensors than R-Type Channels. To find out whether N-type and R-type Ca^{2+} channels are differentially coupled to neurotransmission, we tested the effects of increasing presynaptic Ca^{2+} buffering. When the $-/-$ NMJ were exposed to cell-permeant calcium chelators, EGTA-AM or DM-BAPTA-AM (10 μM), quantal content was significantly reduced (Fig. 3*A*). The impact of DM-BAPTA-AM was significantly greater than the effect of EGTA-AM, as expected from the 100-fold faster on-rate of BAPTA and its more powerful action near the mouth of the channel (47, 48). The effects of the Ca^{2+} buffers on transmission supported by R-type channels and N-type channels were compared (Fig. 3*B*). BAPTA-AM and EGTA-AM both spared the strong reduction of quantal content caused by SNX-482 (1 μM) (Fig. 3*B Left*). In contrast, GVIA produced little or no inhibition after application of either DM-BAPTA-AM or EGTA-AM (Fig. 3*B Right*). The addition of exogenous Ca^{2+} chelators eliminated the reliance on N-type channels, implying that the Ca^{2+} signal from N-type channels acted at a significant distance away from their cytoplasmic mouths. In contrast, R-type channels seemed to be positioned relatively close to the sensing mechanism.

We sought independent confirmation of a differential localization of N- and R-type channels. If R-type channels lie closer to the exocytotic machinery, they might also be positioned more closely to other Ca^{2+} sensors within the active zone, including Ca^{2+}-activated K^+ channels ($I_{K(Ca)}$), which are thought to be intermingled with Ca^{2+} channels at presynaptic release sites (49–52). Perineurial recordings were performed to monitor

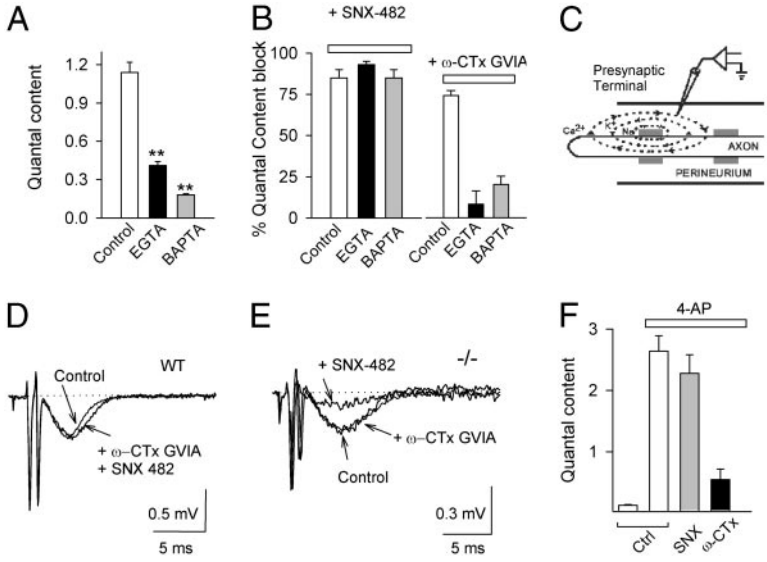

Fig. 3. N-type channels are distant from the Ca^{2+} sensors and more abundant than R-type channels in the α_{1A} −/− NMJ. (*A*) Average quantal content decreased when NMJs were preincubated with 10 μM EGTA-AM (EGTA) or 10 μM DM-BAPTA-AM (BAPTA) compared with DMSO-treated controls. (*B*) R-type channel-dependent transmission was not affected by intracellular Ca^{2+} chelators. Transmission mediated by N-type channels was drastically reduced in the presence of intracellular EGTA or BAPTA, as shown by the weak effect of ω-CTx-GVIA (**, $P < 0.001$). (*C*) Schematic representation of perineurial recording. (*D*) Application of both GVIA and SNX-482 did not affect the $I_{K(Ca)}$ signal in the WT NMJ. (*E*) SNX-482 sharply decreased the $I_{K(Ca)}$ signal in the −/− NMJ, whereas ω-CTx-GVIA (3 μM) was ineffective. (*F*) N-type channels dominate transmission at the mutant NMJ treated with 4-aminopyridine. Large increases in quantal content were observed on application of 4-aminopyridine in control conditions (open bars). Application of 1 μM SNX-482 had no detectable effect on *m*, but 3 μM GVIA strongly reduced it.

endplate $I_{K(Ca)}$ (Fig. 3*C*). Two waves of extracellular negativity were observed, the first corresponding to inward sodium current near the site of recording, the second corresponding to $I_{K(Ca)}$ at the presynaptic terminal, identified by its susceptibility to the selective blocker charybdotoxin (52–54). At the WT NMJ, the $I_{K(Ca)}$ signal is also blocked by AgaIVA, over the same concentration range needed to prevent neurotransmission (24, 25). However, application of N- or R-type blockers produced no reduction of $I_{K(Ca)}$ at WT NMJ, as expected from their lack of involvement in neurosecretion (Fig. 3*D*). In contrast, in perineurial recordings from −/− NMJ, clear inhibitory effects of SNX-482 on the $I_{K(Ca)}$ signal were seen, whereas GVIA was once again ineffective (Fig. 3*E*). Evidently, R-type channels were more favorably positioned relative to $I_{K(Ca)}$ channels, just as in the case of the Ca^{2+} sensor for secretion.

N-Type Ca^{2+} Channels Dominate Transmission at −/− NMJ Treated with 4-AP. Two of our findings might appear to be conflict. The contribution of N-type channels was very strong, inasmuch as GVIA produced >80% inhibition of quantal content, no less than block by SNX-482 (Fig. 2). Yet, transmission supported by N-type channels was more susceptible to exogenous buffers than that generated by R-type channels (Fig. 3*B*), suggesting that the N-type Ca^{2+} signal needed to travel further to reach Ca^{2+} sensors. Were N-type channels simply more numerous, so that they contributed strongly, even if from a distance? To test this, we asked whether N-type channels might be self-sufficient in supporting transmission if their Ca^{2+} influx were augmented by action potential prolongation. α_{1A}−/− NMJs were treated with the K^+ channel blocker 4-aminopyridine (4-AP, 50 μM) to broaden presynaptic spikes (55), and the relative contributions of N- and R-type channels was assessed (Fig. 3*F*). Quantal content was 0.13 ± 0.02 in the presence of 0.5 mM Ca^{2+}/5.5 Mg^{2+}, but rose to 2.7 ± 0.3 after application of 50 μM 4-AP for 30 min (Fig. 3*F*). The effect of the K^+-channel blocker was readily reversible (data not shown). In the presence of 4-AP, 3 μM GVIA continued to exert a strong blocking effect (79 ± 7%), comparable to inhibition in the absence of K^+ channel modulation (82 ± 3%). However, in the presence of 4-AP, SNX-482 (1 μM) reduced quantal content by only 12 ± 12%, in sharp contrast to the strong inhibition observed in the absence of 4-AP (72 ± 6%, $P < 0.001$). The lack of effect of blocking R-type channels when spikes were prolonged was notable given that these channels respond just as strongly as other channel types to prolongation of mock action potentials (55). Apparently, N- and R-type channels differed in their maximal capability for triggering exocytosis at the −/− NMJ. Under favorable conditions, N-type channels were capable of supporting neurotransmission without assistance from R-type channels, suggesting that N-type channels were abundant enough to exert a powerful influence on the Ca^{2+} sensors, even from a greater distance.

Discussion

Elimination of the pore-forming subunit of the P/Q-type channels sets in motion an intricate set of changes, not only in Ca^{2+} channel deployment, but also in synaptic strength, postsynaptic morphology and short-term plasticity. Because transmitter release at the WT NMJ is solely dependent on P/Q-type channels (23–27, 56, 57), the simplest means of safeguarding neurotransmission in the α_{1A} knockout would be a one-to-one replacement of P/Q-type channels by one other channel type. To the contrary, the effects of specific inhibitors indicated that transmission at most if not all release sites must rely jointly on both N- and R-type channels. However, these channels differed considerably in the ways that they supported Ca^{2+}-triggered events. Ca^{2+} influx through R-type channels contributed to transmitter release with minimal interference from exogenous intracellular Ca^{2+} buffers, and was strongly coupled to $I_{K(Ca)}$ channels. Evidently, R-type channels are positioned close to presynaptic Ca^{2+} sensors for secretion or K^+ channel activation, very similar to P/Q-type channels in WT terminals (24, 25). On the contrary, the contribution of N-type channels to transmission was greatly attenuated by the fast on-rate buffer BAPTA, and even the slow on-rate buffer EGTA. Furthermore, N-type channels were not critically involved in the activation of $I_{K(Ca)}$. Both findings suggested that N-type channels were located further away from

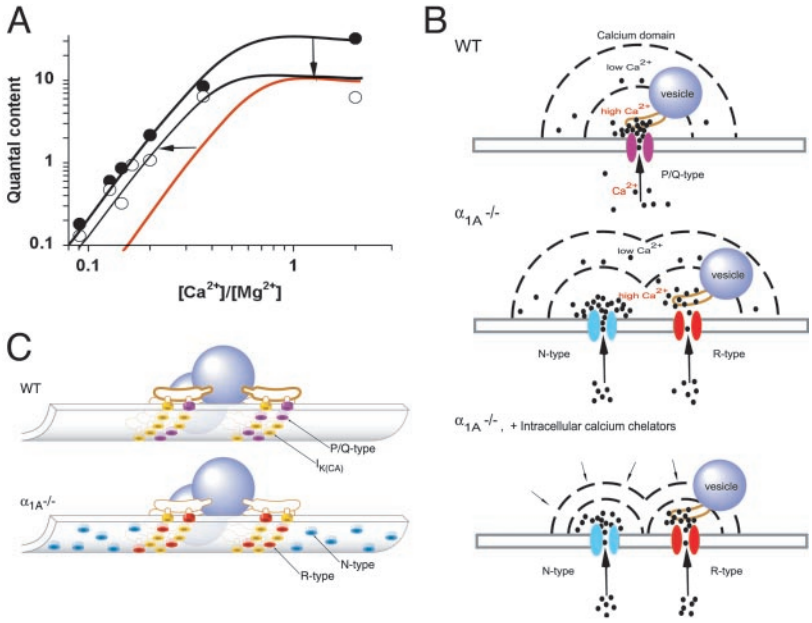

Fig. 4. Schematic representation of presynaptic terminal at the α_{1A} $-/-$ NMJ. (*A*) Calcium dependence of neurotransmission in $-/-$ NMJ. Overall changes include a sharp drop in quantal content at $[Ca^{2+}]_o/[Mg^{2+}]_o = 2$, but little loss of quantal content at $[Ca^{2+}]_o/[Mg^{2+}]_o < 0.2$. This can be described as a uniform scaling down of *m* at all $[Ca^{2+}]_o$ (downward arrow), yielding the red curve, in combination with an increased sensitivity to $[Ca^{2+}]_o/[Mg^{2+}]_o$ (leftward arrow). (*B*) Hypothetical positioning of Ca^{2+} and $I_{K(Ca)}$ channels relative to other active zone structures. (*Upper*) WT NMJ based on description of active zone structures in frog NMJ (20), with modifications appropriate to mammalian terminals, where vesicular fusion occurs in the central zone between double rows of membrane particles (68, 69). Positioning of $I_{K(Ca)}$ channels and P/Q-type channels (purple). (*Lower*) $-/-$ NMJ is hypothesized to contain R-type channels (red) in at least partial substitution for P/Q-type channels (*yellow*), and N-type channels (blue), which are numerous, albeit farther away from Ca^{2+} sensors and vesicle release machinery. (*C*) Microdomains of Ca^{2+} near Ca^{2+} channels in the WT presynaptic terminal (*Top*), in $-/-$ NMJ (*Middle*) and in $-/-$ NMJ in the presence of Ca^{2+} chelators (*Bottom*). GVIA responsiveness is lost because the impact of Ca^{2+} entry through relatively distant N-type channels is blunted by exogenous cytoplasmic Ca^{2+} buffering.

Ca^{2+} sensors for secretion or $K_{(Ca)}$ channel activation than R-type channels (Fig. 3*B*). The greater distance may be counterbalanced by a greater abundance of N-type channels, as inferred from spike broadening experiments (Fig. 3*F*).

These results can be put in context of active zone architecture, as described with electron tomography in frog motor nerve terminals (20). Multiple Ca^{2+} channels and Ca^{2+}-activated K^+ channels (49) are organized by a regular network of presynaptic proteins near fusion-ready vesicles, with several channels linked to each vesicle by rib-like structures. In an extrapolation to active zones at mouse terminals (Fig. 4), we suggest that "slots" for Ca^{2+} channels normally filled by P/Q-type channels can also be occupied by R-type channels. Participation of multiple R-type channels in controlling release at individual sites would fit with the extremely steep dose-dependence of SNX-482 block of R-type-only transmission (Fig. 2).

Even with R- and N-type channels working in combination, the $\alpha_{1A}-/-$ NMJ suffered a morphological and functional deficit that may have contributed to the general weakness of the α_{1A} $-/-$ animals. Imaging of α bungarotoxin-labeled NMJ showed that postsynaptic acetylcholine receptor clusters were $\approx$40% smaller in $-/-$ than in WT, indicating that the overall contact area between pre- and postsynaptic structures was reduced. The predicted reduction in synaptic function fell far short of the $\approx$3-fold deficit in overall release probability we observed at high $[Ca^{2+}]_o/[Mg^{2+}]_o$. Additional changes, beyond the resolution of light microscopy, seem likely.

Two factors govern the overall efficiency of transmission: the unitary probability of release (P_r) of individual release sites and the number of functional release sites (N). Deletion of α_{1A} caused a strong reduction in N, as indicated by a lowering of the saturating value of quantal content, already reached at physiological $[Ca^{2+}]_o$. On its own, a sharp decrease in N should have produced a similar decrease over the entire range of $[Ca^{2+}]_o/[Mg^{2+}]_o$ (Fig. 4*A*, downward arrows leading to red curve). The fact that this did not happen at low $[Ca^{2+}]_o/[Mg^{2+}]_o$ hints at counteracting changes in the properties of the individual release sites that remained functional (Fig. 4*A*; leftward arrows). In principle, this bolstering of unitary release probability could have been attributed to the recruitment of extra N-type channels: the more the extra channels contributed to vesicular release, the more their unitary Ca^{2+} influx would need to be lowered to reduce transmission to the same degree. Alternatively, the Ca^{2+} responsiveness of the Ca^{2+} sensor itself might be enhanced (58). In either case, the $[Ca^{2+}]_o$-dependence of unitary P_r would be displaced toward lower $[Ca^{2+}]_o/[Mg^{2+}]_o$, thereby minimizing the deficit in transmission under conditions of minimal Ca^{2+} entry.

Why is paired-pulse facilitation abolished at the $\alpha_{1A}-/-$ NMJ? Reduction of P_r is generally associated with increased paired-pulse facilitation. Thus, the virtual abolition of PPF at $-/-$ endplates was unexpected. We considered the possibility that compensatory increases in the number of N-type channels might increase the reliability of Ca^{2+} delivery to the point of abolishing facilitation. However, PPF was not rescued by acute blockade of N-type channels (data not shown). A second hypothesis invokes PPF based on priming of Ca^{2+} sensors by residual binding of Ca^{2+} after first-trial failures. PPF would be attenuated by any manipulation that reduces crosstalk between Ca^{2+} channels and Ca^{2+} sensors, such as Ca^{2+} channel toxins (59, 60), intracellular BAPTA (61), or a diminished density of functional release sites, as may occur in the knockout. Yet another possibility is that a Ca^{2+} channel-independent component of compensation contributed to loss of PPF by partially occluding increases in release probability. If P_r at individual sites were already elevated to compensate for a fall in their abundance, further increases in reliability would be accordingly

limited. Rafuse *et al.* (62) found that PPF was abolished by genetic deletion of neural cell adhesion molecule (NCAM), and also discussed the possibility of P_r compensation.

The $\alpha_{1A}-/-$ NMJ was a favorable system for comparisons between all three members of the Ca_v2 family of α_1 subunits in their ability to interact with the release machinery. Our experiments suggest a relative ranking of P/Q>R>N. Discrimination among various Ca^{2+} channel types may also occur during development of the NMJ (60, 61, 63) or recovery of the NMJ from effects of denervation or *Botulinum* toxin treatment (64, 65). Conclusions at the NMJ may also extend to fast transmission at central nervous system synapses, where normal synaptic transmission usually involves multiple Ca^{2+} channels, working together at individual release sites (32–34, 66, 67), though specification of hierarchies among channel types must take into account the availability of the various channel types. It will be interesting to describe effects of α_{1A} deletion at central nervous system synapses where the overall release probability is directly determined by properties of a single release site. Just as changes in synaptic function at the NMJ may contribute to muscle weakness in $\alpha_{1A}-/-$ mice, additional alterations at central synapses may contribute to their ataxia and dystonia.

We are grateful to Dr. U. J. McMahan for helpful discussion, B. Colyear for excellent artwork, and H. Reuter and the Tsien laboratory for comments. This work was supported by Public Health Service Grant NS24067 (to R.W.T.), Ministerio de Salud, Beca Carrillo Oñativia, Universidad de Buenos Aires TW 29, Secretaría de Ciencia, Tecnología e Innovación Productiva, PICT 6220, Argentina, Muscular Dystrophy Association (to O.D.U.), National Creative Initiatives Program, Ministry of Science and Technology, Korea (to H.-S.S.), and Stanford University McCormick Foundation (to E.S.P.-R.). F.J.U. was a United Nations Educational, Scientific and Cultural Organisation/International Union of Pure and Applied Biophysics fellow.

1. Kim, C., Jun, K., Lee, T., Kim, S. S., McEnery, M. W., Chin, H., Kim, H. L., Park, J. M., Kim, D. K., Jung, S. J., *et al.* (2001) *Mol. Cell Neurosci.* **18,** 235–245.
2. Ino, M., Yoshinaga, T., Wakamori, M., Miyamoto, N., Takahashi, E., Sonoda, J., Kagaya, T., Oki, T., Nagasu, T., Nishizawa, Y., *et al.* (2001) *Proc. Natl. Acad. Sci. USA* **98,** 5323–5328.
3. Gautam, M., DeChiara, T. M., Glass, D. J., Yancopoulos, G. D. & Sanes, J. R. (1999) *Brain Res. Dev. Brain Res.* **114,** 171–178.
4. Patton, D. E., West, J. W., Catterall, W. A. & Goldin, A. L. (1992) *Proc. Natl. Acad. Sci. USA* **89,** 10905–10909.
5. Sanes, J. R. & Lichtman, J. W. (2001) *Nat. Rev. Neurosci.* **2,** 791–805.
6. Bean, B. P. (1989) *Nature* **340,** 153–156.
7. Tsien, R. W., Ellinor, P. T. & Horne, W. A. (1991) *Trends Pharmacol. Sci.* **12,** 349–354.
8. Llinas, R., Sugimori, M., Hillman, D. E. & Cherksey, B. (1992) *Trends Neurosci.* **15,** 351–355.
9. Randall, A. & Tsien, R. W. (1995) *J. Neurosci.* **15,** 2995–3012.
10. Mori, Y., Friedrich, T., Kim, M. S., Mikami, A., Nakai, J., Ruth, P., Bosse, E., Hofmann, F., Flockerzi, V., Furuichi, T., *et al.* (1991) *Nature* **350,** 398–402.
11. Ertel, E. A., Campbell, K. P., Harpold, M. M., Hofmann, F., Mori, Y., Perez-Reyes, E., Schwartz, A., Snutch, T. P., Tanabe, T., Birnbaumer, L., *et al.* (2000) *Neuron* **25,** 533–535.
12. Jun, K., Piedras-Renteria, E. S., Smith, S. M., Wheeler, D. B., Lee, S. B., Lee, T. G., Chin, H., Adams, M. E., Scheller, R. H., Tsien, R. W. & Shin, H. S. (1999) *Proc. Natl. Acad. Sci. USA* **96,** 15245–15250.
13. Fletcher, C. F., Tottene, A., Lennon, V. A., Wilson, S. M., Dubel, S. J., Paylor, R., Hosford, D. A., Tessarollo, L., McEnery, M. W., Pietrobon, D., *et al.* (2001) *FASEB J.* **15,** 1288–1290.
14. Miller, R. J. (1997) *Trends Neurosci.* **20,** 189–192.
15. Jen, J. (2000) *Curr. Treat. Options Neurol.* **2,** 429–431.
16. Katz, B. (1969) *The Release of Neural Transmitter Substances* (Liverpool Univ. Press, Liverpool, U.K.).
17. Dodge, F., Jr., & Rahamimoff, R. (1967) *J. Physiol. (London)* **193,** 419–432.
18. Heuser, J. E., Reese, T. S. & Landis, D. M. (1974) *J. Neurocytol.* **3,** 109–131.
19. Heuser, J. E., Reese, T. S., Dennis, M. J., Jan, Y., Jan, L. & Evans, L. (1979) *J. Cell Biol.* **81,** 275–300.
20. Harlow, M. L., Ress, D., Stoschek, A., Marshall, R. M. & McMahan, U. J. (2001) *Nature* **409,** 479–484.
21. Barrett, E. F. & Stevens, C. F. (1972) *J. Physiol. (London)* **227,** 691–708.
22. Sanes, J. R. & Lichtman, J. W. (1999) *Annu. Rev. Neurosci.* **22,** 389–442.
23. Uchitel, O. D., Protti, D. A., Sanchez, V., Cherksey, B. D., Sugimori, M. & Llinas, R. (1992) *Proc. Natl. Acad. Sci. USA* **89,** 3330–3333.
24. Protti, D. A., Sanchez, V. A., Cherksey, B. D., Sugimori, M., Llinas, R. & Uchitel, O. D. (1993) *Ann. N.Y. Acad. Sci.* **681,** 405–407.
25. Protti, D. A. & Uchitel, O. D. (1993) *NeuroReport* **5,** 333–336.
26. Westenbroek, R. E., Sakurai, T., Elliott, E. M., Hell, J. W., Starr, T. V., Snutch, T. P. & Catterall, W. A. (1995) *J. Neurosci.* **15,** 6403–6418.
27. Day, N. C., Wood, S. J., Ince, P. G., Volsen, S. G., Smith, W., Slater, C. R. & Shaw, P. J. (1997) *J. Neurosci.* **17,** 6226–6235.
28. Engel, A. G. (1991) *Ann. N.Y. Acad. Sci.* **635,** 246–258.
29. Sunderland, W. J., Son, Y. J., Miner, J. H., Sanes, J. R. & Carlson, S. S. (2000) *J. Neurosci.* **20,** 1009–1019.
30. Patton, B. L., Cunningham, J. M., Thyboll, J., Kortesmaa, J., Westerblad, H., Edstrom, L., Tryggvason, K. & Sanes, J. R. (2001) *Nat. Neurosci.* **4,** 597–604.
31. Tsien, R. W. & Wheeler, D. B. (1999) in *Calcium as a Cellular Regulator*, eds. Carafoli, E. & Klee, C. B. (Oxford Univ. Press, New York), pp. 171–199.
32. Takahashi, T. & Momiyama, A. (1993) *Nature* **366,** 156–158.
33. Wheeler, D. B., Randall, A. & Tsien, R. W. (1994) *Science* **264,** 107–111.
34. Dunlap, K., Luebke, J. I. & Turner, T. J. (1995) *Trends Neurosci.* **18,** 89–98.
35. Reid, C. A., Bekkers, J. M. & Clements, J. D. (1998) *J. Neurosci.* **18,** 2849–2855.
36. Hubbard, J. L., Llinas, R. & Quastel, D. M. L. (1969) in *Electrophysiological Analysis of Synaptic Transmission*, eds. Hubbard, J. L., Llinas, R. & Quastel, D. M. L. (Edward Arnold, London), pp. 112–173.
37. Cull-Candy, S. G., Miledi, R., Trautmann, A. & Uchitel, O. D. (1980) *J. Physiol. (London)* **299,** 621–638.
38. Urbano, F. J. & Uchitel, O. D. (1999) *Pflugers Arch.* **437,** 523–528.
39. Mallart, A. (1985) *J. Physiol. (London)* **368,** 565–575.
40. Mallart, A. (1985) *J. Physiol. (London)* **368,** 577–591.
41. Betz, W. J. & Bewick, G. S. (1993) *J. Physiol. (London)* **460,** 287–309.
42. Del Castillo, J. & Katz, B. (1954) *J. Physiol. (London)* **124,** 1374–1385.
43. Mallart, A. & Martin, A. R. (1968) *J. Physiol. (London)* **196,** 593–604.
44. Newcomb, R., Szoke, B., Palma, A., Wang, G., Chen, X., Hopkins, W., Cong, R., Miller, J., Urge, L., Tarczy-Hornoch, K., *et al.* (1998) *Biochemistry* **37,** 15353–15362.
45. Tottene, A., Moretti, A. & Pietrobon, D. (1996) *J. Neurosci.* **16,** 6353–6363.
46. Tottene, A., Volsen, S. & Pietrobon, D. (2000) *J. Neurosci.* **20,** 171–178.
47. Neher, E. (1986) in *Calcium Electrogenesis and Neuronal Functioning*, Experimental Brain Research Series, ed. Heinemann, U. (Springer, Berlin), Vol. 14, pp. 1659–1663.
48. Deisseroth, K., Bito, H. & Tsien, R. W. (1996) *Neuron* **16,** 89–101.
49. Robitaille, R., Garcia, M. L., Kaczorowski, G. J. & Charlton, M. P. (1993) *Neuron* **11,** 645–655.
50. Roberts, W. M., Jacobs, R. A. & Hudspeth, A. J. (1990) *J. Neurosci.* **10,** 3664–3684.
51. Llinas, R. & Yarom, Y. (1981) *J. Physiol. (London)* **315,** 569–584.
52. Protti, D. A. & Uchitel, O. D. (1997) *Pflugers Arch.* **434,** 406–412.
53. Anderson, A. J., Harvey, A. L., Rowan, E. G. & Strong, P. N. (1988) *Br. J. Pharmacol.* **95,** 1329–1335.
54. Tabti, N., Bourret, C. & Mallart, A. (1989) *Pflugers Arch.* **413,** 395–400.
55. Wheeler, D. B., Randall, A. & Tsien, R. W. (1996) *J. Neurosci.* **16,** 2226–2237.
56. Protti, D. A., Reisin, R., Mackinley, T. A. & Uchitel, O. D. (1996) *Neurology* **46,** 1391–1396.
57. Bowersox, S. S., Miljanich, G. P., Sugiura, Y., Li, C., Nadasdi, L., Hoffman, B. B., Ramachandran, J. & Ko, C. P. (1995) *J. Pharmacol. Exp. Ther.* **273,** 248–256.
58. Plomp, J. J., Vergouwe, M. N., Van den Maagdenberg, A. M., Ferrari, M. D., Frants, R. R. & Molenaar, P. C. (2000) *Brain* **123,** 463–471.
59. Zengel, J. E., Sosa, M. A. & Poage, R. E. (1993) *Brain Res.* **611,** 25–30.
60. Rosato Siri, M. D. & Uchitel, O. D. (1999) *J. Physiol. (London)* **514,** 533–540.
61. Rosato-Siri, M. D., Piriz, J., Tropper, B. A. & Uchitel, O. D. (2002) *Eur. J. Neurosci.* **15,** 1874–1880.
62. Rafuse, V. F., Polo-Parada, L. & Landmesser, L. T. (2000) *J. Neurosci.* **20,** 6529–6539.
63. Sugiura, Y., Woppmann, A., Miljanich, G. P. & Ko, C. P. (1995) *J. Neurocytol.* **24,** 15–27.
64. Katz, E., Ferro, P. A., Weisz, G. & Uchitel, O. D. (1996) *J. Physiol. (London)* **497,** 687–697.
65. Santafe, M. M., Urbano, F. J., Lanuza, M. A. & Uchitel, O. D. (2000) *Neuroscience* **95,** 227–234.
66. Castillo, P. E., Weisskopf, M. G. & Nicoll, R. A. (1994) *Neuron* **12,** 261–269.
67. Wu, L. G., Westenbroek, R. E., Borst, J. G. G., Catterall, W. A. & Sakmann, B. (1999) *J. Neurosci.* **19,** 726–736.
68. Ellisman, M. H., Rash, J. E., Staehelin, L. A. & Porter, K. R. (1976) *J. Cell Biol.* **68,** 752–774.
69. Walrond, J. P. & Reese, T. S. (1985) *J. Neurosci.* **5,** 1118–1131.